Food Chemistry 304 (2020) 125397

Contents lists available at ScienceDirect

Food Chemistry

journal homepage: www.elsevier.com/locate/foodchem

A highly sensitive competitive immunosensor based on branched polyethyleneimine functionalized reduced graphene oxide and gold nanoparticles modified electrode for detection of melamine

Qunxiang Ren*, Xiaoyan Shen, Yingying Sun, Ronghua Fan, Jun Zhang

Department of Chemistry, Shenyang Medical College, Shenyang 110034, PR China

ARTICLE INFO

Keywords:
Branched polyethyleneimine
Functionalized graphene
Melamine immunosensor
Competitive mode

ABSTRACT

Branched polyethyleneimine functionalized reduced graphene oxide (BPEIGn) was prepared by a one-step reaction, catalyzed by NaOH, using branched polyethyleneimine (BPEI) and graphene oxide (GO) without reductant hydrazine hydrate or sodium borohydride. The branched polyethylenimine acted as both a grafting agent and a reducing agent of GO. An competitive electrochemical immunosensor based on the Au/sodium mercaptopropanesulfonate/BPEIGn/gold nanoparticles/melamine (Au/MPS/BPEIGn/AuNPs/Mel) modified electrode was constructed for the determination of melamine. The double amplification of BPEIGn and AuNPs increased the sensitivity of the sensor. The melamine was detected by differential pulse voltammetry (DPV) in buffer solution (pH 7.4) containing $K_3(Fe(CN)_6]/K_4[Fe(CN)_6]$. Under optimized conditions, the proposed melamine immunosensor showed a linear relationship in the concentration range of 1×10^{-6} to 1 μM, with a detection limit of 2.66×10^{-7} μM.

1. Introduction

Melamine (Mel) is a nitrogen-rich chemical raw material, which is widely used in coatings, plastics, adhesives, textiles, and other industrial production. Melamine is harmful to health and cannot be used for food processing or as a food additive. The protein content in food is generally determined indirectly by the Kjeldahl method, which is based on the determination of the nitrogen content. Since the nitrogen content of melamine is 66.67%, some illegal traders added melamine to milk-containing foods to present a higher content of protein. In 2007, there were many cases of pet poisoning in the United States due to the addition of melamine in pet foods. In 2008, adulteration addition of melamine to milk happen in some milk for enfants produced in China located companies e.g. Sanlu and Nestle. On July 4, 2012, the International Codex Alimentarius Commission, which is responsible for formulating food safety standards, has set a standard for melamine content in liquid milk. The standard requires that the melamine content should not exceed 0.15 mg per kilogram of liquid milk. In 2010, the International Codex Alimentarius Commission stipulated that melamine content should not exceed 1 mg per kilogram of infant formula milk powder. Currently, the national recommended standard detection methods for melamine are high-performance liquid chromatography (HPLC) (Lin et al., 2008; Tan, Li, & Jiang, 2012; Venkatasami & Sowa, 2010), liquid chromatography-mass spectrometry/mass spectrometry (LC-MS/MS) (Andersen, Turinipseed, Karbiwnyk, & Madson, 2007; Rodriguez Mondal, Desmarchelier, Konings, Acheson-Shalom, and Delatour, 2010), gas chromatography-mass spectrometry (GC–MS) (Wu et al., 2013), etc. However, these methods require large and expensive analytical instruments. The analytical methods of electrochemical sensors have the characteristics of low energy consumption, simple equipments and easy miniaturization (Chen et al., 2016; Rao, Chen, Ge, Lu, & Liu, 2017; Pakchin, Ghanbari, Saber, & Omidi, 2018). The electrochemical immunosensor combines immunoassay with electrochemical sensing system by using highly specific binding between antigen and antibody, which has the advantages of high sensitivity and selectivity (Güner, Çevik, Senel, & Alpsoy, 2017). Recently, the analytical technology of electrochemical sensor has developed rapidly and has appeared broad application prospects in the food industry, agriculture, environmental monitoring and medical field. At present, multichannel potentiostats are commercially available. This would mean that calibration procedures could be done rather quickly, as well as multiple unknown samples. So this analysis method will become a very promising detection technology.

The two-dimensional planar structure of graphene together with its excellent electrical conductivity and its large surface area make it an ideal material for electrochemical sensors. (Cao et al., 2016; Er,

* Corresponding author.
E-mail address: chthrqx@hotmail.com (Q. Ren).

https://doi.org/10.1016/j.foodchem.2019.125397
Received 18 March 2019; Received in revised form 6 August 2019; Accepted 18 August 2019
Available online 19 August 2019
0308-8146/

Çelikkan, & Erk, 2017; Farid, Goudini, Piri, Zamani, & Saadati, 2016; Ren, Feng, Fan, Ge, & Sun, 2016). The graphene is very stable, and the chemical reaction is inert. The van der Waals forces between the layers are relatively strong, and the agglomeration occurs easily. The properties mentioned above are not conducive to the research and application of graphene. Since graphene oxide (GO) contains many active groups such as hydroxyl, carboxyl and epoxy groups (Shanmugharaj, Yoon, Yang, & Ryu, 2013; Yang et al., 2009), the GO can be covalently functionalized by other molecules. The functionalized graphene showed good dispersibility, which can improve the availability of graphene. The water-soluble branched polyethyleneimine (BPEI) can provide many active amino groups, which can covalently bond with the epoxy groups on the GO via the nucleophilic ring-opening reaction. The polyethyleneimine functionalized reduced graphene oxide was generally prepared by a two-step reaction. First, the polyethyleneimine and GO were mixed and stirred for 24 h at a certain temperature, then the hydrazine hydrate or sodium borohydride was added to the mixture and stirred for several hours. (Li, Chen, & Shi, 2017; Shan et al., 2013).

The first aim of this study is to prepare branched polyethyleneimine functionalized reduced graphene oxide (BPEIGn) with good dispersibility and strong conductivity by a one-step reaction of graphene oxide and branched polyethyleneimine under alkaline condition without reductant hydrazine hydrate or sodium borohydride, which evades the aggregation of graphene because the complicated synthesis process easily leads to the aggregation of graphene. In addition to being a grafting agent of GO, the branched polyethyleneimine also acts as a reductant of GO.

The BPEIGn has a larger specific surface and a bigger space charge layer than a two-dimensional sheet of graphene, so it shows excellent electrochemical activity. Melamine shows a rigid planar structure that is not easily deformed, while the branched polyethyleneimine exhibits a strong flexible structure that is easily deformed to form the space-matched configuration. This flexible structure of the branched polyethyleneimine and its rich amino groups can enhance its interaction with melamine. Therefore, the second aim of this study is to use the synthesized BPEIGn to construct a highly sensitive competitive melamine immunosensor based on the Au/sodium mercaptopropanesulfonate/BPEIGn/AuNPs/melamine (Au/MPS/BPEIGn/AuNPs/Mel) modified electrode, and realize the detection of melamine in real samples. The melamine was detected by differential pulse voltammetry (DPV) in buffer solution (pH 7.4) containing $K_3(Fe(CN)_6]/K_4[Fe(CN)_6]$. The free melamine in the solution and the melamine immobilized on the electrode surface competed to react with the melamine antibody in the solution, and the peak current of DPV varied with melamine concentration in the solution.

2. Experiments

2.1. Reagents and materials

All chemicals were of analytical grade. The branched polyethyleneimine (Mw = 25000), bovine serum albumin (BSA) and melamine were obtained from Sigma-Aldrich. Natural graphite flakes, lysine, valine, leucine, proline, lactose, vitamin A, vitamin C, $CaCI_2$, KCI, chloroauric acid, sodium citrate, sodium 3-mercaptopropanesulfonate, trichloroacetic acid, and methanol purchased from the Sinopharm Chemical Reagent Co., Ltd. Melamine monoclonal antibody came from Beijing Bioss Biotechnology Co., Ltd. The liquid milk produced by Shenyang Huishan Company and the whole milk powder produced by Shanghai Guangming Company were purchased from Resources Vanguard Supermarket in Shenyang of China. All of the solutions were prepared using double-distilled water.

2.2. Apparatus

All electrochemical experiments were carried out on a CHI 760E electrochemical workstation (Chenhua, China) with a traditional three-electrode cell using a saturated calomel electrode as the reference electrode, a modified Au disk electrode with a diameter of 2 mm as the working electrode, and a platinum wire as the counter electrode. 10 gold disc electrodes were purchased from Shanghai Chenhua. Transmission electron microscopy (TEM; Hitachi H-7650, Japan) was used to observe the morphology of the AuNPs, GO and BPEIGn. X-ray photoelectron spectroscopy (XPS) spectra were acquired on an ESCALAB250 X-ray photoelectron spectrometer (Thermo VG, USA). Fourier transform infrared spectroscopy (FTIR) spectra were recorded using a Perkin Elmer 2000 spectrophotometer (PE, USA) using KBr pellets. Raman spectra of the GO and BPEIGn were recorded on a DXR smart Raman spectrometer (Thermo Fisher, USA). The synthetic reaction was carried out on a DF-101S collector-type thermostat heating magnetic stirrer (Yuhua, China).

2.3. Preparation of BPEIGn

The graphene oxide was prepared using the modified Hummers method (Marcano et al., 2010). 30 mg of the graphene oxide was dispersed in 30 mL of double-distilled water and sonicated for 1 hour to obtain a uniformly distributed graphene oxide solution. 3 mL of 0.25 mol/L NaOH and 3 mL of 5% branched polyethyleneimine were added dropwise to the above solution successively, and the reaction mixture was stirred for 20 h at 70 °C. The mixture was then centrifuged and washed three times with double-distilled water to remove the impurities and the excess physically absorbed BPEI. A portion of the centrifuged product was freeze-dried to obtain BPEIGn powder sample for spectral testing. The remainder was redispersed in double-distilled water to form a homogeneous solution. No precipitation occurred after the dispersion was stored for a month.

2.4. Preparation of gold nanoparticles

The glassware was soaked in aqua regia, rinsed with deionized water and dried with baking. One hundred milliliters of 0.01% chloroauric acid was heated to boiling in a round-bottom flask and stirred at maximum speed using a magnetic stirrer. When the first drop of liquid reflux occurred in the condenser, 4 mL of freshly prepared 1% sodium citrate solution was added. The color changed from pale to blue and then to transparent wine red. Boiling was continued for 15 min, and the sample was stirred until it cooled to room temperature.

2.5. Assembly of the modified electrode

The gold electrode was polished with 0.3 μm and 0.05 μm of Al_2O_3 powder and sonicated in double-distilled water and ethanol solution alternately. The electrode was dried with nitrogen steam. 6 μL of 20 mM sodium 3-mercaptopropanesulfonate solution was added onto the surface of the treated electrode and dried at room temperature, washed with phosphate buffer solution (PBS) (pH 7.4) solution and dried with nitrogen. After that, 6 μL of 1 mg/mL BPEIGn, 6 μL of AuNPs and 6 μL of 0.2 mg/mL melamine were successively modified onto the surface of the electrode with the same procedure. Finally, the modified electrode was immersed in 1% bovine serum albumin (BSA) solution for 1 hour at room temperature to block possible remaining active sites. The preparation process of the modified electrode is shown in Fig. 1. The modified electrode was denoted as Au/MPS/BPEIGn/AuNPs/Mel.

2.6. Real sample pre-treatment

The liquid milk and milk powder were pretreated with the general procedure (Cao et al., 2009; Guo et al., 2014; Liu, Xiao, Cui, & Wang, 2015). 5 mL liquid milk (or 2 g milk powder) was first mixed with 5 mL of 0.06 mol L^{-1} trichloroacetic acid and 20 mL of methanol. After 8 min shaking and 8 min ultrasonic treatment, the solution was centrifuged at

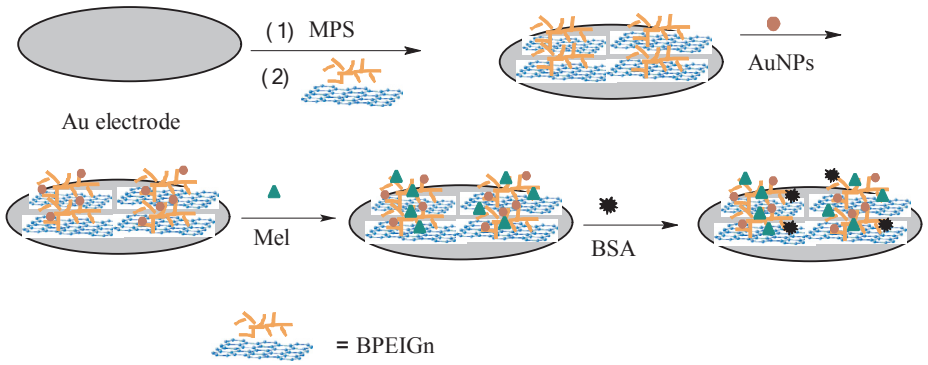

Fig. 1. Stepwise assembly process of the Au/MPS/BPEIGn/AuNPs/Mel electrode.

10000 rpm for 8 min, and the supernatant was filtered. Next, the filtrate was condensed to obtain a total volume of 5 mL and filtered through a 0.45 μm filter membrane.

3. Results and discussion

3.1. Characterization of BPEIGn

The dispersions of AuNPs, GO and BPEIGn treated by ultrasound were dripped onto copper meshes respectively, and their micro-morphology was observed by TEM. As shown in Fig. 2, the gold nanoparticles are well dispersed and spherical with a particle size of about 10–15 nm. The GO nanosheets exhibit a wrinkled morphology, and similar wrinkles can be found in BPEIGn. The appearance of BPEIGn revealed that the resulting BPEIGn exhibited an excellent dispersity in doubly-distilled water.

The FT-IR spectra of GO and BPEIGn are shown in Fig. 3A. The peaks of the FTIR spectrum of GO are similar to that reported in the previous references (Sheshmani & Amini, 2013; Tian et al., 2014). GO exhibited characteristic peaks at 3367, 1731, 1621, 1222, 1051 and 853 cm^{-1}, which were attributed to O—H stretching vibration, C═O stretching vibration, the stretching vibration of aromatic ring C═C, C—O stretching vibration, C—O—C symmetric stretching vibration, and C—O—C asymmetric stretching vibration, respectively. The characteristic peaks of oxygen-containing groups at 1731 cm^{-1}, 1222 cm^{-1} and 853 cm^{-1} disappeared in the FT-IR spectrum of BPEIGn. This result suggested that GO was reduced. The FT-IR spectra of BPEI and BPEIGn are shown in Fig. 3B. The FT-IR spectrum of BPEIGn showed the characteristic peaks of BPEI and the assignment is as follows: 3281 cm^{-1} (N—H stretching vibration peak), 2942 cm^{-1} and 2823 cm^{-1} (–CH_2–symmetric and asymmetric stretching vibration of BPEI chain), 1569 cm^{-1} (N—H in-plane bending vibration), 1432 cm^{-1} (CH_2 in-plane bending vibration), 1295–1039 cm^{-1} (C—N stretching vibration) and 764 cm^{-1} (N—H out-of-plane bending vibration). The presence of the characteristic peaks of the BPEI in the FT-IR spectrum of BPEIGn suggested that BPEI was grafted onto the reduced GO.

The XPS spectra of GO and BPEIGn are shown in Fig. 3C. Two sharp peaks are observed at 284 eV (C1s) and 532 eV (O1s). The peak intensity ratio C1s/O1s of the XPS spectrum of BPEIGn is higher than that of graphene oxide. The increase in the ratio is attributed to the removal of most oxygen-containing groups. The appearance of N1s peak (399 eV) in the XPS spectrum of BPEIGn indicates that the branched polyethyleneimine was grafted onto GO. To better investigate the deoxygenation of the branched polyethyleneimine on GO, the C (1 s) spectra of GO and BPEIGn were deconvoluted. The C1s spectrum of GO was deconvoluted into four peaks as follows: C—C and C═C (284.5 eV), C—O (286.6 eV), C═O (287.8 eV) and O═C–OH (289.0 eV) (Akhavan, Ghaderi, Aghayee, Fereydooni, & Talebi, 2012). It can be seen from Fig. 3(D and E) that the peak areas of O═C–OH, C═O and C—O of BPEIGn are significantly decreased compared with GO. Such a decrease is attributed to the removal of the oxygen-containing groups. The 285.6 eV peak in the C (1 s) spectrum of BPEIGn was attributed to the C—N bond. Actually, the presence of nitrogen in BPEIGn was also confirmed by the survey XPS spectrum of BPEIGn.

Raman spectroscopy was used to characterize BPEIGn further, as shown in Fig. 3F. The Raman spectra of GO and BPEIGn display the D peak at about1346 cm^{-1} and the G peak at about 1590 cm^{-1}. The value of the I_D/I_G intensity ratio is a measure of the local defects or disorders of graphene (Akhavan & Ghaderi, 2012). It was found that the I_D/I_G ratio (1.05) of BPEIGn is higher than the I_D/I_G ratio (0.92) of GO. The results showed that the local defects or disorders were produced in the carbon network after the branched polyethyleneimine functionalization of GO. Moreover, the Raman spectrum of GO displays a 2D peak at 2710 cm^{-1}, which is sensitive to the graphene sheet stacking. The 2D

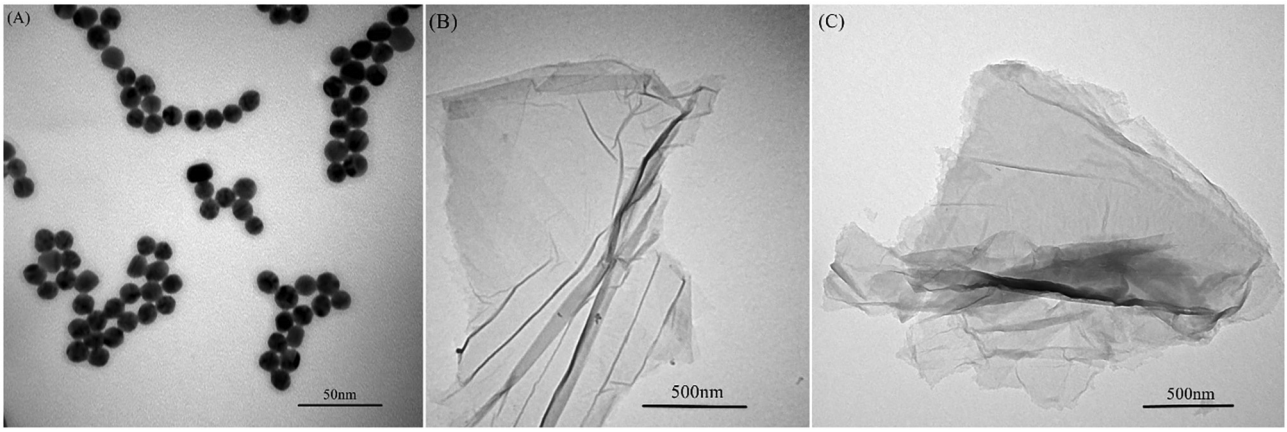

Fig. 2. TEM images of the AuNPs (A), GO (B) and BPEIGn (C).

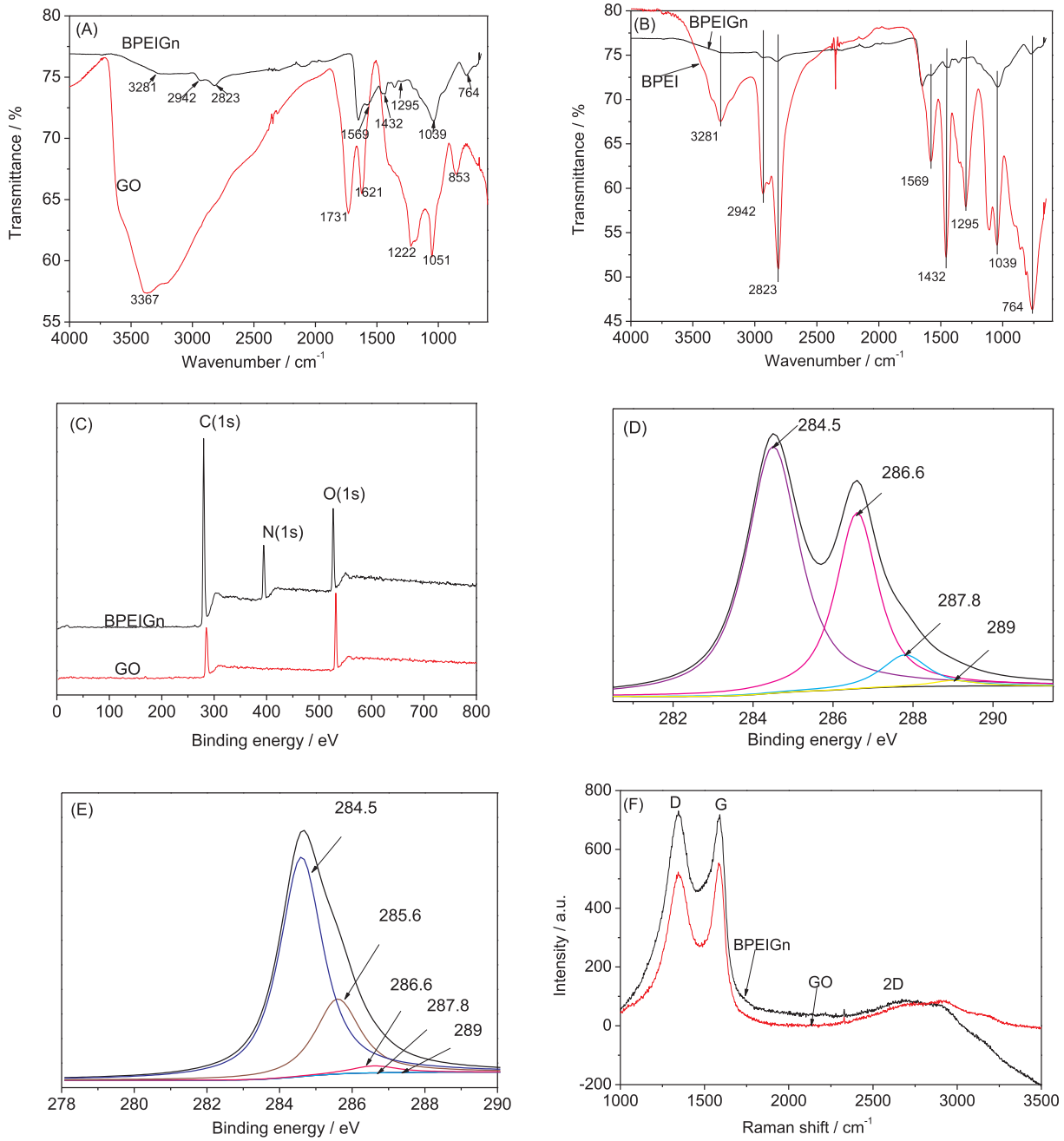

Fig. 3. (A) FTIR spectra of GO and BPEIGn; (B) FTIR spectra of BPEI and BPEIGn; (C) The survey XPS spectra of GO and BPEIGn; (D) The high-resolution XPS of C(1S) of GO; (E) The high-resolution XPS of C(1S) of BPEIGn; (F) The Raman spectra of GO and BPEIGn.

peak for the BPEIGn shifted to low wavenumber (2670 cm^{-1}), revealing that the distance between the layers of graphene sheets was increased after the branched polyethyleneimine was grafted onto the graphene oxide.

3.2. The assembly mechanism and characterization of the modified electrode Au/MPS/BPEIGn/AuNPs/Mel

At first, the negatively charged sodium 3-mercaptopropanesulfonate was assembled onto the Au electrode through the Au-S bond, and the positively charged BPEIGn was absorbed on the surface of the electrode through electrostatic interaction. The surface of BPEIGn was crowded with many amino groups and positive charges, and the negatively charged AuNPs were immobilized onto the electrode by the covalent interaction and electrostatic adsorption. Subsequently, melamine was attached to the electrode surface by the formation of hydrogen bonds with the polyethyleneimine. The flexible structure of the branched polyethyleneimine and its rich amino groups enhanced its interaction with melamine. Finally, bovine serum albumin (BSA) was used to block the non-specific absorption sites to obtain the melamine immunosensor modified electrode.

The cyclic voltammetry. (CV) curves of different modified electrodes are shown in Fig. 4A. The cyclic voltammetric curve of the bare electrode in PBS (pH 7.4) containing 1.0 mmol/L $K_3[Fe(CN)_6]/K_4[Fe(CN)_6]$ showed a pair of obvious redox peaks (a). When sodium 3-mercaptopropanesulfonate was modified on the electrode, the peak current decreased (b). After the electrode was modified by branched polyethyleneimine functionalized graphene, the peak current increased significantly (c), which implies that the BPEIGn has excellent electrochemical activity and can enhance electron transfer. The excellent

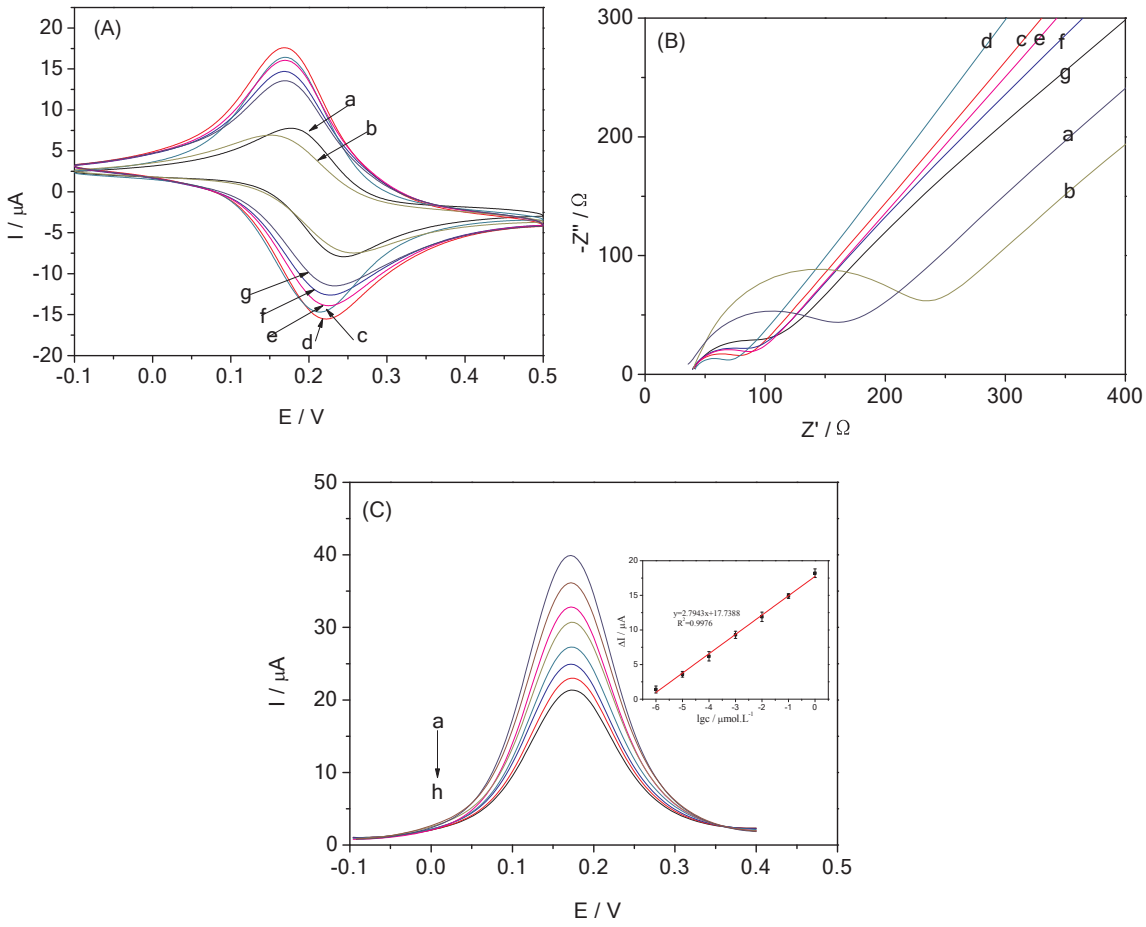

Fig. 4. (A) Cyclic voltammograms of the same electrode at different stages in PBS (pH 7.4) containing 1.0 mmol/L $K_3[Fe(CN)_6]/K_4[Fe(CN)_6]$ at a scan rate of 50 mV/s; (B) Electrochemical impedance spectra of the same electrode at different stages in PBS (pH 7.4) containing 5.0 mmol/L $K_3[Fe(CN)_6]/K_4[Fe(CN)_6]$. a. Bare Au electrode, b. Au/MPS electrode, c. Au/MPS/BPEIGn electrode, d. Au/MPS/BPEIGn/AuNPs electrode, e. Au/MPS/BPEIGn/AuNPs/Mel electrode, f. Au/MPS/BPEIGn/AuNPs/Mel/BSA electrode, g. Au/MPS/BPEIGn/AuNPs/Mel/BSA-antibody. (C) DPV curves of the Au/MPS/BPEIGn/AuNPs/Mel electrode after the incubation in 0.1 mol/L PBS solution (pH 7.4) containing the same concentration of melamine antibody and various concentrations of melamine. a–h: 1, 1×10^{-1}, 1×10^{-2}, 1×10^{-3}, 1×10^{-4}, 1×10^{-5}, 1×10^{-6} and 0 μmol L^{-1} melamine solution (from top to bottom). The inset is the calibration curve.

electrochemical properties of the BPEIGn depend on its structure. The BPEIGn has a larger specific surface and a bigger space charge layer than a two-dimensional sheet of graphene. The modification of AuNPs to the surface of the electrode further increased the peak current (d). The peak current decreased (e) after melamine was modified onto the electrode because melamine hindered the electron transfer. The peak current further decreased (f) after the nonspecific binding sites were blocked by BSA (a non-conductive substance). After the prepared modified electrode was placed in the incubation solution containing melamine antibody, the peak current decreased (g) because the binding of the antibody and the melamine on the electrode hindered the electron transfer. This also suggested that the melamine molecule had been modified on the electrode.

Fig. 4B shows the electrochemical impedance spectroscopy (EIS) of different modified electrodes in PBS (pH 7.4) containing 5.0 mmol/L $K_3[Fe(CN)_6]/K_4[Fe(CN)_6]$. Compared with the impedance of the bare electrode (a), the value of the impedance of the modified electrode with sodium mercaptopropionate increased (b). The impedance values of the electrode after the modification of BPEIGn (c) and AuNPs (d) gradually decreased, indicating that BPEIGn and AuNPs facilitated the transport of electrons. The modification of melamine (e) and blocking of BSA (f) increased the impedance values, suggesting that melamine and BSA impeded the electron transfer. The impedance value further increased (g) after the electrode was placed in the solution containing the melamine antibody. The results of the electrochemical impedance spectra were consistent with those of the cyclic voltammograms, indicating that the immunosensor had been successfully prepared.

3.3. Detection of melamine

The detection of the melamine was realized by the differential pulse voltammetry method based on the specific binding of the melamine monoclonal antibody and melamine. The incubation solution consisted of a PBS (pH 7.4) solution containing a series of different concentrations of melamine (1, 1×10^{-1}, 1×10^{-2}, 1×10^{-3}, 1×10^{-4}, 1×10^{-5}, 1×10^{-6} and 0 μmol L^{-1}) and the same concentration of melamine antibody. The modified electrode was immersed in the incubation solution for 50 min, in this period, the free melamine in the solution and the melamine immobilized on the electrode surface competed to react with the melamine antibody in the solution. After the incubation for 50 minutes, the electrode was washed by the PBS (pH 7.4) solution and dried with nitrogen for the test of DPV. The DPV peak current increased as the concentration of melamine in the incubation solution increased (Fig. 4C). The difference in response current $\Delta I = I - I_0$ was proportional to the logarithm of the melamine concentration between $1 \times 10^{-6} \sim 1$ μmol L^{-1} (Where I_0 is the DPV response current of the modified electrode after incubation in the PBS solution containing only melamine antibody, and I is the DPV response current of the modified electrode after incubation in the PBS solution containing melamine antibody and melamine). The linear regression

equation was $\Delta I = 2.7943 \log c + 17.7388$, with a correlation coefficient of 0.9976. According to the recommendation (Long & Winefordner, 1983) of International Union of Pure and Applied Chemistry (IUPAC), the detection limit was calculated based on the $3S_B/m$ criterion (where m is the slope of the calibration curve and S_B is the standard deviation of the blank in the absence of the melamine, n = 10). The detection limit of the proposed sensor was determined to be 2.66×10^{-7} μmol L^{-1} by relating $3S_B$ to a concentration value divided by the slope of the calibration curve.

3.4. Optimization of immunization conditions

The incubation time of immune reaction was optimized. The modified electrode was incubated for 0, 10, 20, 30, 40, 50 and 60 min in the incubation solution containing the same concentration of antibody and the DPV was measured. As illustrated in Fig. S1, the DPV peak current of the melamine sensor decreased with an increase in incubation time. The response current kept unchanged after 50 min, indicating that the balance of the antigen–antibody reaction was achieved at 50 min, which was determined as the optimal immune reaction time

The effect of the antibody mass concentration in the incubation solution on the immune reaction was studied. As shown in Fig. S2, the Au/MPS/BPEIGn/AuNPs/Mel modified electrode was incubated for 50 min in 100 μL of 0.1 mol/L PBS solution containing different concentrations of the antibody at 37 ℃, and the DPV peak current was significantly reduced as the mass concentration of the antibody rose from 0 μg/mL to 5 μg/mL, and the decline of the peak current was barely noticeable between 5–8 μg/mL. The results indicated that when the concentration of the antibody was greater than 5 μg/mL, the binding sites were basically saturated. For the competitive immunosensor, the chosen antibody concentration should be lower than the concentration that caused the saturation of the binding sites. If the antibody concentration in the incubation solution was too high, the competitive reaction could not be detected because the amount of antibody was sufficient to react with the melamine in the incubation solution and immobilized on the electrode surface. Then 4 μg/mL was selected as the optimal antibody concentration.

3.5. Method evaluation

The analytical parameters of the proposed biosensor and the other melamine biosensors previously reported are compared and summarized as shown in Table 1. The results show that the constructed melamine biosensor has a wider linear range and a low detection limit.

The repeatability, stability and regeneration of the melamine immunosensor were studied. Five individual Au disc electrodes prepared under the same conditions were used to test the melamine samples. The RSD of the samples was 4.1%, indicating that the proposed sensor showed good reproducibility. The immunosensor was continuously scanned for 20 cycles in the $K_3[Fe(CN)_6]/K_4[Fe(CN)_6]$ solution by the CV, and the peak current was almost unchanged. The immunosensor electrode was stored at 4 ℃, and the differential pulse voltammetry was measured every 5 days. The results showed that the current response of the immunosensor decreased by only 8.1% after one month, indicating that the sensor exhibited good stability. The incubated modified electrode was soaked in 0.1 mol/L glycine-HCl (pH 2.0) for 15 min, and the antibody adsorbed on the electrode surface was washed away to regenerate the sensor.

Liquid milk and milk powder usually contain amino acids, vitamins, ions and lactose. In order to assess the anti-interference ability of the immunosensor, the effects of these coexisting substances (such as lysine, valine, leucine, proline, lactose, vitamin A, vitamin C, $CaCl_2$ and KCl, etc.) on the test of melamine were studied. The DPV was measured after the incubination of the modified electrode in the PBS buffer solution (pH 7.4) containing 4 μg/mL melamine antibody and 1 μmol L^{-1} melamine or with 50 μmol L^{-1} lysine, valine, leucine, proline, lactose, vitamin A, vitamin C, $CaCl_2$ and KCl, respectively. As shown in Fig. S3, the concentration of the interfering substance was 50 times that of the Mel, and the DPV peak current change for the mixture of the Mel and other individual interfering substance was less than 4% of the peak current for the Mel solution without interfering substance, indicating that the immunosensor showed a good selectivity.

3.6. Practical application

The practicality of the immunosensor based on the fabricated Au/MPS/BPEIGn/AuNPs/Mel modified electrode has been assessed by the determination of the melamine in the real sample. The liquid milk and milk powder were bought from a supermarket and pretreated according to the procedure described in 2.6. The melamine in the liquid milk and milk powder was determined by a standard addition method, and the results are listed in Table 2. As can be seen from Table 2, the recoveries are in the range from 98.7% to 104.0%, and the RSD is below 3.4%. Thus, the accurate determination of melamine in liquid milk and milk powder and good recoveries indicated excellent practical feasibility of the sensor based on the fabricated Au/MPS/BPEIGn/AuNPs/Mel modified electrode.

4. Conclusion

The branched polyethyleneimine functionalized reduced graphene oxide was prepared by a one-step reaction from graphene oxide and branched polyethyleneimine under alkaline condition. In this reaction, the branched polyethyleneimine served as both a grafting agent and a reducing agent of GO. In this study, an electrochemical immunosensor based on the Au/MPS/BPEIGn/AuNPs/Mel modified electrode was constructed, and the detection of melamine was realized. The double amplification of BPEIGn and AuNPs increased the sensitivity of the sensor. Under the optimized experimental conditions, the constructed electrochemical immunosensor showed a wide linear range and low detection limit. The proposed sensor showed excellent practical feasibility.

Table 1
Comparisons of the linear range and detection limit of this work with the other methods for the determination of melamine.

Materials and method	Linear range(μM)	Detection limit(μM)	Refs.
CNT–IL/MIP	0.4–9.2	0.11	Liu et al. (2015)
GCE/Poly(para-aminobenzoic acid)	4.0–450	0.36	Liu et al. (2011)
Imprinted sol–gel electrochemical sensor	0.63–110	0.068	Xu et al. (2014)
GCE/Au@PANI NPs	1×10^{-5}–10	1.39×10^{-6}	Rao et al. (2017)
GCE/AuNPs/rGO	5×10^{-3}–0.05	1.0×10^{-3}	Chen, Cheng, Li, Zhang, and Zhao (2015)
Screen-printed carbon electrode	5–200	0.8	Liao, Chen, Chang, and Zen (2011)
GCE/ascorbic acid as probe	0.01–0.350	1.5×10^{-3}	Li et al. (2012)
GCE/RUDS/CMWCNTs/Nafion	5.0×10^{-7}–1.0×10^{-1}	1.0×10^{-7}	Chen et al. (2016)
GCE/MWCNTs/Chitosan	9.9×10^{-3}–1.9×10^{-1}	3.0×10^{-3}	Zhao, Liu, Li, Dang, and Li (2012)
Silver nanoclusters	0.1–0.03	0.004	He, Li, Fu, and Jin (2016)
Au/MPS/BPEIGn/AuNPs/Mel	1×10^{-6}–1	2.66×10^{-7}	This work

Table 2
Results of the determination of the melamine in real samples.

Sample	Added (nM)	Detected(nM)	Recovery (%)	RSD (%)(n = 3)
Liquid milk	0	0	–	–
	10	10.4	104.0	2.6
	50	50.2	100.4	3.1
	100	99.6	99.6	1.9
Milk powder	0	0	-	
	10	10.2	102.0	2.3
	50	49.6	99.2	3.4
	100	98.7	98.7	2.9

Declaration of Competing Interest

The authors declare that they have no known competing financial interests or personal relationships that could have appeared to influence the work reported in this paper.

Acknowledgments

This work was supported financially by the Liaoning Natural Science Foundation (No. 20170540876) and the Science and Technology Program of Shenyang Medical College (No. 20161010)

Appendix A. Supplementary data

Supplementary data to this article can be found online at https://doi.org/10.1016/j.foodchem.2019.125397.

References

Akhavan, O., & Ghaderi, E. (2012). Escherichia coli bacteria reduce graphene oxide to bactericidal graphene in a self-limiting manner. *Carbon, 50*, 1853–1860.
Akhavan, O., Ghaderi, E., Aghayee, S., Fereydooni, Y., & Talebi, A. (2012). The use of a glucose-reduced graphene oxide suspension for photothermal cancer therapy. *Journal of Materials Chemistry, 22*, 13773–13781.
Andersen, W. C., Turinipseed, S. B., Karbiwnyk, C. M., & Madson, M. R. (2007). Determination of melamine residues in catfish tissue by triple quadrupole LC–MS–MS with HILIC chromatography. *Laboratory Information Bulletin, 23*, 4396.
Cao, Q., Zhao, H., Zeng, L., Wang, J., Wang, R., Qiu, X., et al. (2009). Electrochemical determination of melamine using oligonucleotides modified gold electrodes. *Talanta, 80*, 484–488.
Cao, X., Xu, H., Ding, S., Ye, Y., Ge, X., & Yu, L. (2016). Electrochemical determination of sulfide in fruits using alizarin–reduced graphene oxide nanosheets modified electrode. *Food Chemistry, 194*, 1224–1229.
Chen, N., Cheng, Y., Li, C., Zhang, C., & Zhao, K. (2015). Determination of melamine in food contact materials using an electrode modified with gold nanoparticles and reduced graphene oxide. *Microchimica Acta, 182*, 1967–1975.
Chen, X., Lian, S., Ma, Y., Peng, A., Tian, X., Huang, Z., et al. (2016). Electrochemiluminescence sensor for melamine based on a $Ru(bpy)_3^{2+}$-doped silica nanoparticles/carboxylic acid functionalized multi-walled carbon nanotubes/Nafion composite film modified electrode. *Talanta, 146*, 844–850.
Er, E., Çelikkan, H., & Erk, N. (2017). An ultra-sensitive 2D electrochemical sensor based on a PtNPs@graphene/Nafion nanocomposite for determination of α_1-AR antagonist silodosin in human plasma. *Analytical Methods, 9*, 3782–3789.
Farid, M. M., Goudini, L., Piri, F., Zamani, A., & Saadati, F. (2016). Molecular imprinting method for fabricating novel glucose sensor: Polyvinyl acetate electrode reinforced by MnO_2/CuO loaded on graphene oxide nanoparticles. *Food Chemistry, 194*, 61–67.
Guo, Z., Xu, X., Li, J., Liu, Y., Zhang, J., & Yang, C. (2014). Ordered mesoporous carbon as electrode modification material for selective and sensitive electrochemical sensing of melamine. *Sensors and Actuators B: Chemical, 200*, 101–108.
Güner, A., Çevik, E., Senel, M., & Alpsoy, L. (2017). An electrochemical immunosensor for sensitive detection of Escherichia coli O157:H7 by using chitosan, MWCNT, polypyrrole with gold nanoparticles hybrid sensing platform. *Food Chemistry, 229*, 358–365.
He, R., Li, M., Fu, Y., & Jin, L. (2016). Silver nanoclusters functionalized by chromotropic acid and layered double hydroxides for turn-on detection of melamine. *Journal of Materials Chemistry C, 4*, 6104–6109.
Li, J., Kuang, D., Feng, Y., Zhang, F., Xu, Z., & Liu, M. (2012). A novel electrochemical method for sensitive detection of melamine in infant formula and milk using ascorbic acid as recognition element. *Bulletin of the Korean Chemical Society, 33*, 2499–2507.
Li, N., Chen, J., & Shi, Y. P. (2017). Magnetic polyethyleneimine functionalized reduced graphene oxide as a novel magnetic solid-phase extraction adsorbent for the determination of polar acidic herbicides in rice. *Analytica Chimica Acta, 949*, 23–34.
Liao, C. W., Chen, Y. R., Chang, J. L., & Zen, J. M. (2011). Single-run electrochemical determination of melamine in dairy products and pet foods. *Journal of Agricultural and Food Chemistry, 59*, 9782–9787.
Lin, M., He, L., Awika, J., Yang, L., Ledoux, D. R., & Li, H. (2008). Detection of melamine in gluten, chicken feed and processed foods using surface-enhanced Raman Spectroscopy and HPLC. *Journal of Food Science, 73*, 129–134.
Liu, B., Xiao, B., Cui, L., & Wang, M. (2015). Molecularly imprinted electrochemical sensor for the highly selective and sensitive determination of melamine. *Materials Science and Engineering C, 55*, 457–461.
Liu, Y. T., Deng, J., Xiao, X. L., Ding, L., Yuan, Y. L., Li, H., et al. (2011). Electrochemical sensor based on a poly(para-aminobenzoic acid) film modified glassy carbon electrode for the determination of melamine in milk. *Electrochimica Acta, 56*, 4595–4602.
Long, G. L., & Winefordner, J. D. (1983). Limit of detection. A closer look at the IUPAC definition. *Analytical Chemistry, 55*, 712A–724A.
Marcano, D. C., Kosynkin, D. V., Berlin, J. M., Sinitskii, A., Sun, Z., Slesarev, A., et al. (2010). Improved synthesis of graphene oxide. *ACS Nano, 4*, 4806–4814.
Pakchin, P. S., Ghanbari, H., Saber, R., & Omidi, Y. (2018). Electrochemical immunosensor based on chitosan-gold nanoparticle/carbon nanotube as a platform and lactate oxidase as a label for detection of CA125 oncomarker. *Biosensors and Bioelectronics, 122*, 68–74.
Rao, H., Chen, M., Ge, H., Lu, Z., & Liu, X. (2017). A novel electrochemical sensor based on Au@PANI composites film modified glassy carbon electrode binding molecular imprinting technique for the determination of melamine. *Biosensors and Bioelectronics, 87*, 1029–1035.
Ren, Q., Feng, L., Fan, R., Ge, X., & Sun, Y. (2016). Water-dispersible triethylenetetramine-functionalized graphene: Preparation, characterization and application as an amperometric glucose sensor. *Materials Science and Engineering C, 68*, 308–316.
Rodriguez Mondal, A. M., Desmarchelier, A., Konings, E., Acheson-Shalom, R., & Delatour, T. (2010). Liquid chromatography-tandem mass spectrometry (LC-MS/MS) method extension to quantify simultaneously melamine and cyanuric acid in egg powder and soy protein in addition to milk products. *Journal of Agricultural and Food Chemistry, 58*, 11574–11579.
Shan, C., Wang, L., Han, D., Li, F., Zhang, Q., Zhang, X., et al. (2013). Polyethyleneimine-functionalized graphene and its layer-by-layer assembly with Prussian blue. *Thin Solid Films, 534*, 572–576.
Shanmugharaj, A. M., Yoon, J. H., Yang, W. J., & Ryu, S. H. (2013). Synthesis, characterization, and surface wettability properties of amine functionalized graphene oxide films with varying amine chain lengths. *Journal of Colloid and Interface Science, 401*, 148–154.
Sheshmani, S., & Amini, R. (2013). Preparation and characterization of some graphene based nanocomposite materials. *Carbohydrate Polymers, 95*, 348–359.
Tan, J., Li, R., & Jiang, Z. T. (2012). Determination of Melamine in Liquid Milk and Milk Powder by Titania-Based Ligand-Exchange Hydrophilic Interaction Liquid Chromatography. *Food Analytical Methods, 5*, 1062–1069.
Tian, J., Yuan, P. X., Shan, D., Ding, S. N., Zhang, G. Y., & Zhang, X. J. (2014). Biosensing platform based on graphene oxide via self-assembly induced by synergic interactions. *Analytical Biochemistry, 460*, 16–21.
Venkatasami, G., & Sowa, J. R. (2010). A rapid, acetonitrile-free, HPLC method for determination of melamine in infant formula. *Analytica Chimica Acta, 665*, 227–230.
Wu, X., Wang, P., Yang, D., Wang, L., Shen, X., & Zhu, C. (2013). Simultaneous determination of melamine and cyanuric acid in dairy; products by mixed-mode solid phase extraction and GC-MS. *Food Control, 30*, 545–548.
Xu, G., Zhang, H., Zhong, M., Zhang, T., Lu, X., & Kan, X. (2014). Imprinted sol–gel electrochemical sensor for melamine direct recognition and detection. *Journal of Electroanalytical Chemistry, 713*, 112–118.
Yang, H., Shan, C., Li, F., Han, D., Zhang, Q., & Niu, L. (2009). Covalent functionalization of polydisperse chemically-converted graphene sheets with amine-terminated ionic liquid. *Chemical Communications, 45*, 3880–3882.
Zhao, T., Liu, L., Li, G., Dang, A., & Li, T. (2012). Electrochemical Determination of Melamine with a Glassy Carbon Electrode Coated with a Multi-Wall Carbon Nanotube/Chitosan Composite. *Journal of The Electrochemical Society, 159*, K141–K145.